Diamond & Related Materials 19 (2010) 389–396

Contents lists available at ScienceDirect

Diamond & Related Materials

journal homepage: www.elsevier.com/locate/diamond

Simulations of polycrystalline CVD diamond film growth using a simplified Monte Carlo model

P.W. May [a,*], N.L. Allan [a], M.N.R. Ashfold [a], J.C. Richley [a], Yu.A. Mankelevich [b]

[a] School of Chemistry, University of Bristol, Bristol BS8 1TS, United Kingdom
[b] Skobel'tsyn Institute of Nuclear Physics, Moscow State University, Vorob'evy gory, Moscow 119991, Russia

ARTICLE INFO

Available online 6 November 2009

Keywords:
CVD diamond growth
Modelling
Nucleation
Nanodiamond

ABSTRACT

A simple 1-dimensional Monte Carlo (MC) model has been developed to simulate the chemical vapour deposition (CVD) of a diamond (100) surface. The model considers adsorption, etching/desorption, lattice incorporation, and surface migration along and across the dimer rows. The reaction probabilities are taken from experimental or theoretical literature values for standard CVD diamond conditions. Renucleation events believed to be due to reactive adsorbates, such as C atoms or CN groups, were modelled by creating random surface defects which form a critical nucleus upon which to nucleate a new layer. By assuming that migrating C species that encounter these surface defects add to the growing surface by templating either from the underlying layer or from the surface defect, and with suitable colour coding, the evolution of different grains has been modelled. On increasing the probability of creating surface defects, the number of grains increases while their mean size decreases. This simulates the film morphology changing from that of single crystal diamond to microcrystalline, nanocrystalline and finally ultrananocrystalline diamond. With the formation of such defects which can act as renucleation points turned off, but using random seed crystals, the films develop a columnar structure similar to that observed for heteroepitaxial microcrystalline diamond.

1. Introduction

Chemical vapour deposition (CVD) of diamond is a maturing technology that is beginning to find commercial applications in electronics, cutting tools, medical coatings and optics [1], and shows great potential for quantum computing [2], biosensing [3], field emission devices and thermionic solar cells [4]. The CVD process involves the gas phase decomposition of a gas mixture containing a small quantity of a hydrocarbon in excess hydrogen [5]. A typical gas mixture uses 1% CH_4 in H_2, and this produces polycrystalline films with grain sizes in the micron or tens of micron range, depending upon growth conditions, substrate properties and growth time. By increasing the ratio of methane in the standard CH_4/H_2 gas mixture from 1% to ~5%, the grain size of the films decreases, and eventually becomes of the order of hundreds down to tens of nm. Such nanocrystalline diamond (NCD) films (often termed 'cauliflower' or 'ballas' diamond) are smoother than the microcrystalline ones, but have larger numbers of grain boundaries that contain substantial graphitic impurities. With further addition of CH_4 the films become graphitic. Diamond films with even smaller grain sizes (~2–5 nm) are often called 'ultrananocrystalline' diamond (UNCD) films [6,7], and most reports of the deposition of UNCD films describe using a microwave (MW) plasma CVD reactor and gas mixture of 1%CH_4 in Ar, usually with addition of 1–5% H_2 [8]. At the other end of the size scale, single crystal diamonds (SCD) up to several carats (1 carat = 0.2 g) in weight have recently been successfully grown in high power MW CVD reactors using 1%–12%CH_4/H_2 mixtures, sometimes with small additions of N_2 or O_2 [9–12].

However, to obtain a diamond film with the desired morphology combined with controlled electronic and mechanical properties requires a detailed understanding of the many parameters affecting growth, such as the substrate temperature, gas mixture, process pressure, etc. The difficulty with this is that, even 20 years after diamond CVD was first developed, the exact details of the growth mechanism remain controversial. The so-called 'standard growth mechanism' [13] developed in the early 1990s is a robust description of the general CVD diamond process. In this model, atomic H, created by thermal or electron-impact dissociation of H_2, is the driving force behind all the chemistry. It is widely accepted [14,15] that the main growth species in standard diamond CVD is the CH_3 radical, which adds to the diamond surface following hydrogen abstraction by H atoms. An elevated substrate temperature (typically >700 °C) allows migration of the adsorbed C species until they meet a step-edge and add to the diamond lattice. Another role for the atomic H is to etch back into the gas phase any adsorbed carbon groups that have deposited as non-diamond phases. It is believed that hydrocarbons C_xH_y with 2 or more carbons ($x \geq 2$) are prevented from contributing to the growth by the 'β-scission' reaction which is a rapid, low energy, efficient process that stops the build up of polymer chains on the growing surface. Diamond growth is

* Corresponding author.
E-mail address: paul.may@bris.ac.uk (P.W. May).

0925-9635/$ – see front matter © 2009 Elsevier B.V. All rights reserved.
doi:10.1016/j.diamond.2009.10.030

therefore seen as competition between etching and deposition, with carbons being added to the diamond on an atom-by-atom basis.

This standard growth model predicts some of the general features of the observed morphology, plus growth rates to within an order of magnitude. However, the model has problems predicting the crystallite size and whether the resulting film will be UNCD, NCD or even SCD. Furthermore, a mechanism for renucleation of a new layer is not covered by the standard model. Impurities, such as N_2, in the gas phase have been suggested as catalysts for nucleation [16], as have larger hydrocarbons, such as C_2H_y or C_3H_y, and defect formation at biradical sites [17].

Our group recently developed a modified version of the standard growth model which considers the effects of all the C_1 hydrocarbon radicals (CH_3, CH_2, CH and C atoms) on both monoradical and biradical sites on a (100) diamond surface [18]. In this model, for most standard deposition conditions (i.e. with high atomic H concentrations at the growth surface) diamond growth is still dominated by CH_3 adding to monoradical surface sites, leading to large crystals. Addition of CH_3 to the biradical sites also leads to large crystals, since the unused surface dangling bond is rapidly hydrogenated during the process of converting the CH_3 adduct into a CH_2 surface group [19]. However, the increased relative contribution of the biradical mechanism enhances the probability that other reactive hydrocarbon species (C_2, C_2H, etc.) from the gas can add to these biradical sites. Such reactive species then have the opportunity to cross-link on the surface, creating a strongly-bonded (maybe even non-etchable) defect. This surface defect could act as either a renucleation point for a new epitaxial layer, or, if it is misaligned with the existing lattice, a new crystallite growing in a different direction to that of the main bulk. This last possibility is often termed 'renucleation', and leads to a decrease in the average crystal size. If renucleation occurs frequently, the crystallite size can drop from mm to μm, and eventually to nm, and the films are termed SCD, MCD and (U)NCD, accordingly.

As well as CH_3, addition of the other less abundant but highly reactive C_1 species, particularly atomic C, to either type of radical site at high H atom concentration, can also be a route to growth, since the dangling bonds on the adduct would be rapidly hydrogenated converting the adduct into CH_3. However, at low H atom concentration, the dangling bonds on the adduct can cross-link to lattice sites, again leading to renucleation and subsequent smaller crystal sizes. Additionally, evidence from very recent quantum-mechanical *ab initio* modelling [20] shows that some C_1 species, in particular C atoms, can directly insert into the C–H surface bonds of diamond with a low or even zero energy barrier. This may be yet another mechanism for the creation of surface defects.

Our growth model [18] also relies upon surface migration of CH_2 groups along and across the reconstructed dimer rows in order to predict growth rates to within a factor of two of experimental observations. Using the model we derived expressions for the fraction of monoradical sites, R, and biradical sites, R^2, based upon the substrate temperature, T_s, and the concentrations of H and H_2 above the surface. Under typical CVD diamond conditions with $T_s \sim 900$ °C and 1%CH_4/H_2, $R \sim 0.1$. This means that ~10% of the surface carbon atoms support monoradical sites, while 1% of the surface consists of biradical sites (a radical site on two adjacent C atoms). The model also generated an expression for the average crystallite size $\langle d \rangle$ which depends upon T_s and crucially upon the square of the ratio of all the C_1 hydrocarbon concentrations to that of atomic H, i.e. $([CH_y]/[H])^2$. The expression for $\langle d \rangle$ predicted values that agreed well with experiments that ranged from a few nm corresponding to UNCD [21] to mm for single crystal diamond [22].

Despite these successes, evidence for surface migration, nucleation processes, the effects of gas impurities and gas-surface reactions are sparse and mostly circumstantial. To investigate these ideas we developed a simplified one-dimensional Monte Carlo (MC) model of the growth of diamond films [23]. Although the model was only 1D, the interplay between adsorption, etching/desorption and addition to the lattice were modelled successfully using known or estimated values for the rates of each process. For typical CVD diamond conditions, the model predicted growth rates of ~1 μm h^{-1}, consistent with experiment. Various other growth processes were also predicted, such as step-edge growth, a large positive value for the Ehrlich–Schwoebel potential for migrating species attempting to migrate off the top of step-edges leading to atomic-scale 'wedding cake' structures, and it also showed that β-scission is not as important for determining the surface morphology as previously envisaged. A major assumption of the MC model is that surface defects can be modelled assigning values for the probability of their appearance following certain surface processes, such as migration and adsorption. Such immobile, unetchable surface defects act as critical nuclei, allowing the nucleation of new layers, and thus a greatly increased growth rate when the rate-determining step for growth is new layer nucleation. The rationale for this is that one possible fate for a migrating C species, if the multiple bond-breaking and bond-reforming processes that occur during each migration step [24] were to go awry, is to trigger the formation of an immobile surface defect. This could occur, for example, as a result of H abstraction converting the benign migrating CH_2 group into a more reactive CH or atomic C moiety. Most of these isolated surface defects would simply be etched back into the gas phase, leaving behind a pristine diamond surface. But some may survive long enough to act as a nucleating point for a new layer, which may or may not follow the orientation of the underlying lattice.

Similar static surface defects could also be formed when CH_3 adds to the less abundant (~1% of the surface) biradical sites, since the resulting adduct will find itself with a reactive dangling bond immediately adjacent to it. The most likely fates for this dangling bond are either (i) ring closure, (ii) rapid hydrogen termination by reaction with the abundant gas-phase atomic H, or (iii) for CH_3 to attach to it. Pathways (i) and (iii) may produce surface structures inconsistent with the underlying lattice, and so may act as the defect to trigger renucleation, while process (ii) simply turns the biradical site into a monoradical site. However, an alternative fourth pathway is for a reactive gas phase species such as C_2, C_2H, C, etc., to add to this dangling bond and then reconstruct into a surface defect. Although this may be a minority process due to the low abundance of these species, every time it occurs it can create a renucleation point, leading to a decrease in the average crystallite size [18].

Another defect-forming process involves adsorbing unsaturated atomic C or CH species, since their 'dangling bonds' permit unusual surface bonding. For standard diamond CVD conditions, the concentrations of C and CH striking the surface are usually negligible compared to that for CH_3. But under H-poor conditions, such as those used for UNCD growth, they can become significant contributors to the growth [25]. A further possibility for initiating a new layer from a static surface defect is from impurities in the gas phase, such as N_2 [16], since this reacts to form CN species in the gas phase [26] which can then add to the surface to form the critical nucleus.

By whichever mechanism they are created, such static surface defects could act as the critical nucleus needed to help start a new layer, or instigate the (re)nucleation of a new crystallite, ultimately leading to a polycrystalline film. In this paper we shall present the results of extending the existing MC program to simulate polycrystalline diamond growth, and show that experimental observations such as columnar growth, renucleation, and the homogeneous arrangement of crystallites in NCD and UNCD films can be modelled using this simple approach.

2. Experimental

The full model for the MC program is given in detail in Ref. [23] and therefore we shall give only a brief description here. One requirement for our model was that we wished to be able to view the growth of the diamond surface in 'real time' using a desktop PC. The program was written using Microsoft QuickBasic, which although not optimised for

modern PCs, was easy to program and had the required graphical capability built in.

In many respects our model resembles the standard 1D kinetic MC models that have been used to model crystal growth and thin film molecular beam epitaxy (MBE) for a decade or more [27]. However, our version contains a number of parameters specific to diamond growth, as well as several unique subroutines written specially to test diamond-growth-specific mechanisms, such as β-scission.

In our 1D MC model, the diamond lattice is represented in only 2 dimensions, as a cross-section, with the top (growing) surface positioned towards the top of the screen. Each C atom is represented by a square block within the lattice, with different coloured blocks representing different 'types' of carbon bonding. Carbons that are fully bonded into the diamond lattice are coloured dark-blue whereas carbons that are temporarily adsorbed on the surface are green.

The grid has a maximum size of 600×400, but for speed of computation 2×2 blocks were used for most simulations, making the effective grid size 300×200. At the start of the program, a flat horizontal surface of dark-blue blocks is defined at the bottom of the screen to represent a single crystal diamond substrate. A random number, R_1 $(0\leq R_1<1)$, is then generated and compared to the probability of a new incoming block, P_{new}, which is calculated based on the known flux of CH_3 radicals towards the surface under typical CVD conditions (see later). If $R_1<P_{\text{new}}$ a new incoming green-coloured block is chosen at a random horizontal position at the top of the screen, and then allowed to drop vertically until it meets the surface, whereupon it temporarily adsorbs at this position. This block represents a generic C_1 adsorbing unit, which is most probably CH_3 but could be species such as C, CH, CH_2 or even CN. The adsorbed green block then has a number of possible pathways, depending upon the local morphology where it landed, and each possible fate is tested sequentially at every time-step of the program.

A green block landing in a position with no blocks immediately either to its left or right has the possibility to simply desorb (or be etched) back into the gas phase. Another random number, R_2, is generated and compared with the probability of desorption/etching, P_{desorb} (see later). If $R_2<P_{\text{desorb}}$ the block desorbs and is removed. If the block remains on the surface, a subsequent possible fate for it is to stick permanently to form a static, unetchable defect. A third random number R_3 is generated and compared with the probability for direct-defect formation, $P_{\text{dir-def}}$. If $R_3<P_{\text{dir-def}}$ the block is given a random colour (chosen from 10 possibilities) and attaches permanently to the lattice. (The value of 10 comes from the limitations of using 8-bit QBASIC as a programming language which allows only 16 colours, 6 of which are already defined in the program to represent the diamond lattice, migrating blocks, defects, the background, etc. Ideally, at least 100 colours should be available to avoid duplication, and this improvement may be included in a more advanced version of the program in the future.) If the block does not add to the lattice, desorb or permanently stick as a defect, then a final possibility is that it migrates. A fourth random number, R_4, is generated and compared to the probability of migration, P_{mig}. If $R_4<P_{\text{mig}}$ the block will jump left or right one space, with equal chance. If the block still finds itself with no immediate neighbours in its new position, it might either form a static defect (with probability $P_{\text{jump-def}}$), in which case it is given another random colour (chosen as before), or it may remain temporarily adsorbed ready to migrate again at the next time-step. $P_{\text{jump-def}}$ can be different from $P_{\text{dir-def}}$ since the mechanisms forming the static surface defect might be different in each case.

Apart from defect formation, 'normal' additions to the lattice occur when an adsorbing or migrating block encounters a step-edge, i.e. a neighbouring block of any colour. In this case the moving block will permanently bond to it, change colour (following the rules given below) and remain there for the duration of the program. In this model, the diamond lattice itself is considered unetchable, so once a moving block has added to the lattice, it cannot subsequently be removed (except in the special case of a β-scission reaction, see below). The colour for the newly-added block is chosen based on the assumption that it would template itself to either the underlying block or the side block, with a probability P_{below} determining the branching ratio between these two possibilities. If the colour of the block below and the block to the side of the newly-added block are the same, then the new block simply becomes this new colour. However, if the colours are different, a new random number R_5 is generated and compared to P_{below}. If $R_5<P_{\text{below}}$ the block becomes the colour of the block below; otherwise it becomes the colour of the block to the side. With no theoretical data upon which to base an estimate for P_{below}, a value of 0.5 has been chosen as default, giving equal probability to each possibility. But this value has also been varied to see its effect upon crystallite size and shape.

Three other features of the model need to be mentioned. First, this 1D model assumes that the 'normal critical nucleus' for diamond growth is two adjacent blocks. This is defined as the smallest immobile, unetchable surface feature that provides step-edges suitable for propagating layer growth. Under standard growth conditions a normal 2-block critical nucleus can be formed by (i) an Eley-Rideal-type process, where an incoming green block adsorbs directly next to a previously adsorbed block causing both of them to bond together, or (ii) a Langmuir–Hinshelwood-type process where two adsorbed green blocks migrate next to one another and fuse together. These two processes form the basis for new layer nucleation in the absence of defects (*i.e.* when $P_{\text{jump-def}}=P_{\text{jump-def}}=0$). Note, surface defects form the special case of a critical nucleus of size 1 block.

Second, β-scission is modelled by scanning the surface blocks after every time-step and identifying and deleting any 2-block pillars that may have arisen as a result of blocks landing or migrating. The probability that β-scission occurs is chosen to be 1, meaning that β-scission happens every time it is possible at each time-step. Second, there is the issue of blocks migrating off the top of step-edges. From arguments outlined in Ref. [23] we have adopted the 'cowards' scenario as the default process, which means that migrating blocks cannot jump off the top of step-edges, consistent with a positive Ehrlich–Schwoebel barrier for this process.

The program was cycled until it was stopped manually or until a preset number of layers (typically 150 to provide statistical invariance) had grown, at which point the data were saved. Depending upon the choice of probabilities for the various events, the program took only a few minutes to grow 150 layers (on a Pentium 4 PC). Thus, the evolution of the surface morphology could be directly followed on the computer screen, giving insight into which parameters control different aspects of growth.

In a MC model of this type, the time-step is chosen to be equal to or faster than the fastest process occurring. This fastest process (which for these process conditions turns out to be surface migration) is normalised to give a probability of 1 (or less if required) to occur at each time-

Table 1
The probabilities per time-step for each of the processes in the model normalised to the fastest process [23].

Process	Probability symbol	Normalised probability
Surface migration along and across (100) dimer rows.	P_{mig}	1
CH_3 impact on radical site.	P_{new}	5×10^{-6}
Desorption/etching.	P_{desorb}	0.05
Surface defect creation following direct impact.	$P_{\text{dir-def}}$	0.0005
Surface defect creation following migration.	$P_{\text{jump-def}}$	0.0005
Combined surface defect creation (renucleation).	P_{renucl}	0.0005
β-scission (taken to be the same as that of migration, i.e. it happens at every time-step).	P_{beta}	1
Addition of a migrating C group to a step-edge.	$P_{\text{add-step}}$	1
Templating on the underlying block compared to the side-edge block.	P_{below}	0.5

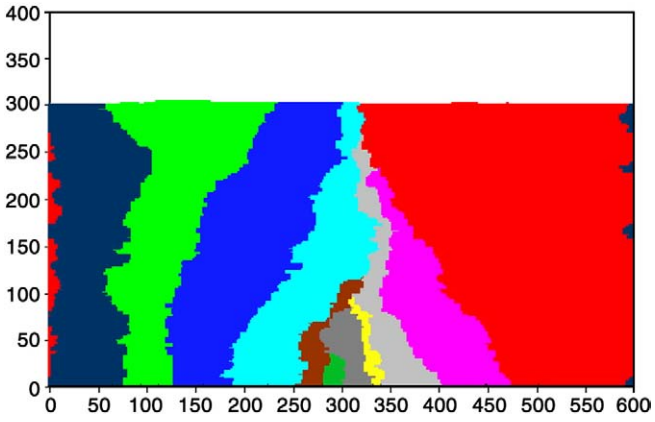

Fig. 1. Simulation of columnar polycrystalline diamond growth using 10 randomly spaced diamond seed crystals on a (100) non-diamond substrate, with 2×2 blocks and the probability values given in Table 1.

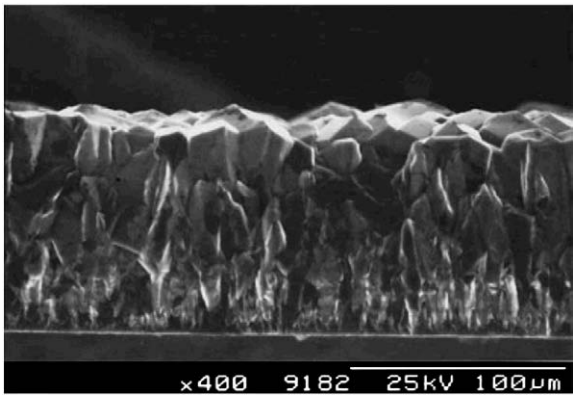

Fig. 2. Scanning electron micrograph of a cross-section through a microcrystalline CVD diamond film grown on (100) Si showing the columnar structure.

step, and the other processes are assigned probabilities based on their relative rates with respect to this fastest one. In order to simplify matters, we shall assume that the growth conditions are fixed for standard polycrystalline CVD grown at a substrate temperature of ~900 °C using 1%CH_4/H_2 at a process pressure of ~20 Torr [18]. We also assume that CH_3 is the only species important for growth of diamond, although other species such as atomic C, CH, C_2, etc., will be important for renucleation processes. The values chosen for the probabilities for the various processes, based upon the known or estimated relative rates for each process, are discussed in detail in Ref. [23], and are given in Table 1. The maximum growth rate will occur when there is 100% utilisation of all the incoming C species and no loss mechanisms (no desorption/etching or β-scission). At an impact rate of 8 s^{-1} per radical site and a C–C bond length of 1.5 Å we obtain a maximum growth rate for typical diamond deposition conditions of ~4.3 μm h^{-1}. This agrees quite well with experimental growth rates which have values ~1 μm h^{-1} for these conditions — smaller than the calculated maximum due to the active loss mechanisms.

For this paper, two different growth scenarios are investigated. In the first, renucleation is 'turned off' ($P_{\text{dir-def}} = P_{\text{jump-def}} = 0$), but the non-diamond surface is 'seeded' with a chosen number of randomly positioned diamond nuclei. This scenario simulates the growth of heteroepitaxial CVD diamond films which nucleate upon scratches or seed crystals resulting from manual or ultrasonic abrasion prior to growth. One difference between the simulation and real deposition is that in the simulation the seed crystals are considered to lie on top of the (100) substrate surface with their <100> direction parallel to this substrate, whereas in reality they would be lying at random orientations. The second scenario uses diamond (100) as the substrate (*i.e.* homoepitaxial growth), but instead of seed crystals, renucleation is 'turned on' by making both $P_{\text{dir-def}}$ and $P_{\text{jump-def}} > 0$.

3. Results

Using the values given in Table 1 the program achieved its goals of simulating the growth of 150 layers of diamond in a few minutes, with the morphology continuously evolving on the screen. The type of growth seen, the growth rate and the film morphology are a complicated function of the probabilities used, and these have been discussed in our previous paper for single crystal diamond growth [23]. Here we concentrate on the effects of renucleation and defect formation upon film growth characteristics.

(a) Columnar growth of microcrystalline diamond

Fig. 1 shows the results of the simulation with renucleation turned off ($P_{\text{dir-def}} = P_{\text{jump-def}} = 0$) and 10 randomly positioned seed crystals on a non-diamond surface. With renucleation turned off the growth from each seed was single domain, and each crystallite grew until it met its neighbours, at which point the crystallite islands coalesced into a continuous film. Subsequent growth resulted in a columnar appearance to the crystallites, with the apparent crystal size increasing with growth time. Some crystallites have been overgrown by the others, so that the number of crystallites surviving after 150 layers of growth was only 5 out of the original 10. The probability of a crystallite surviving depended inversely upon the distance between its originating seed crystal and any nearest neighbouring seed crystals. Due to the step-edge growth mechanism, growth from a seed crystal spreads laterally until it meets the growth from another crystal. Thus, crystallites with neighbouring seeds in close proximity become thin and narrow, whilst those with more

Fig. 3. 3D tomographic electron backscattered detection images of the cross-section through a CVD diamond film grown with 1%CH_4/H_2 at 900 °C (from the Max-Planck-Institut für Eisenforschung). The orientations of different grains have been colour-coded based upon their alignment with the axis parallel to the growth direction. Reprinted with permission of the authors from Ref. [28], copyright 2009, Wiley.

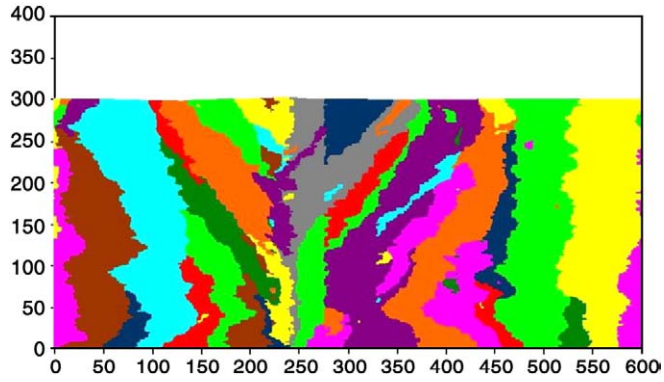

Fig. 4. Simulation of columnar polycrystalline diamond growth using 17 randomly spaced diamond seed crystals on a non-diamond (100) substrate, with 1×1 blocks and the probability values given in Table 1, except with renucleation turned on with P_{renucl} = 0.00001. The columnar structure still dominates, however new crystallites have formed throughout the film thickness as a result of renucleation.

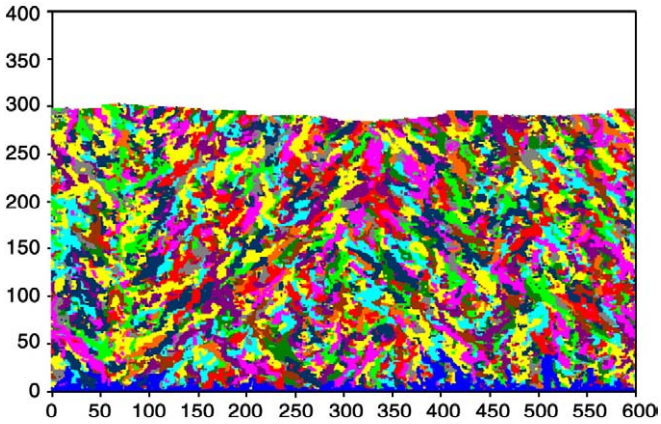

Fig. 6. Simulation of nanocrystalline diamond growth on a single crystal diamond (100) surface (coloured dark-blue) using 1×1 blocks and the probability values given in Table 1, except with P_{renucl} = 0.001.

distant neighbours can develop a wide base before growing upward producing a thicker column. From the law of probabilities, the thicker columns stand a greater chance of survival than thinner ones. Comparison between Fig. 1 and the electron micrograph cross-section of a CVD diamond film grown under similar CVD conditions (1%CH_4/H_2 in a hot filament reactor following manual abrasion with 1–3 μm diamond grit) shown in Fig. 2, shows that many of the growth features have been simulated remarkably accurately. Despite the different length scales (the simulation is for 150 atomic layers whereas the SEM is for a 100 μm-thick film), features such as the columnar nature of the growth, the overgrowth of slower-growing crystallites, and the increasing size of crystallites with film thickness have all been reproduced in the simulation. The simulation predicts that the crystallites are not straight-edged - as is often depicted in schematic diagrams of columnar growth – but have grain boundaries that are, instead, more diffuse and poorly-defined. We should add a note of caution here. The experimental data are taken from a cross-section of a fully 3D film. Thus, some columnar crystallites will protrude out of the plane of the cross-section, whilst others will protrude into this plane. However, the cross-section would show these as crystallites appearing to start or end part-way up the film. Thus, at present our simulation cannot distinguish between new crystallites that start as a result of renucleation events, and those that are a direct result of 3D geometry. This matter will be addressed when we convert our 1D model into a fully 2D model in future work.

The grain-boundaries are difficult to pick out in SEM images such as Fig. 2, but Fig. 3 shows a cross-sectional image of a similar diamond film that has been obtained using electron backscattered detection tomography, with each crystallite colour-coded [28,29]. In this figure, all the grain boundaries can be distinguished, and the shape, orientation, and appearance of the crystallites closely resemble the irregular shapes predicted by Fig. 1. One notable difference is that in Fig. 3 some new grains are formed high up in the cross-section as a result of renucleation processes discussed in section (b) below, which are not included in this simulation. By adding renucleation with a suitable value for P_{renucl}, formation of these new grains can be simulated and an even closer resemblance between simulation and experiment can be obtained, see Fig. 4.

Fig. 5 shows a plot of the total number of grains as a function of the number of initial seed crystals, and the result is a near-straight line, as might be expected. Also shown is the number of grains that survive to reach the surface 150 layers above the seeds. This value rises to ~5 and then plateaus at this value as many of the grains are overgrown. The value of 5 is simply a function of the grid size, the resolution (2×2) and the height of the film, and would be different if any of these parameters were varied.

(b) Nanocrystalline diamond

Using a simulated diamond (100) surface (dark-blue blocks) without seed crystals, and with renucleation turned on (i.e. $P_{dir\text{-}def}$ and $P_{jump\text{-}def}$>0) results in a decrease in the grain size. For these simulations $P_{dir\text{-}def}$ and $P_{jump\text{-}def}$ had the same value, and we call this combined defect probability P_{renucl}. Fig. 6 shows a simulation of a film grown using P_{renucl} = 0.001. The film is now composed of a homogeneous matrix of small, randomly-shaped grains. All signs of the columnar growth seen previously in Fig. 1 have disappeared, although some dark-blue blocks representing crystallites that have

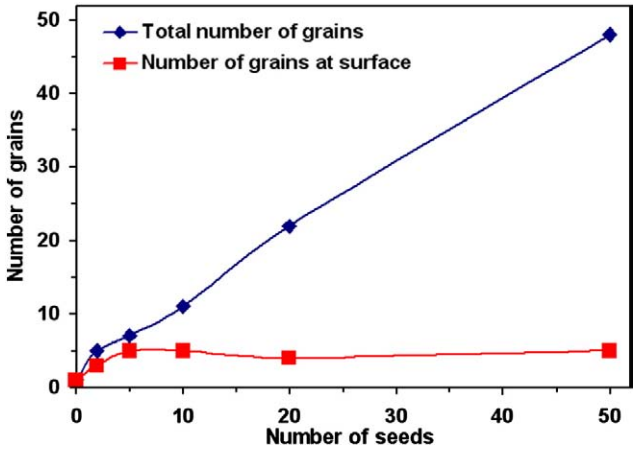

Fig. 5. Total number of grains and number of surface grains plotted as a function of the number of seed crystals.

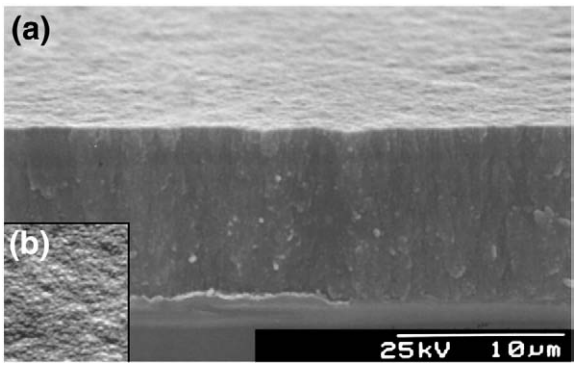

Fig. 7. Scanning electron micrograph of a nanocrystalline diamond film grown in a hot filament CVD reactor using 4%CH_4/H_2 gas on a Si (100) substrate. (a) Cross-section, (b) inset, top view at the same scale.

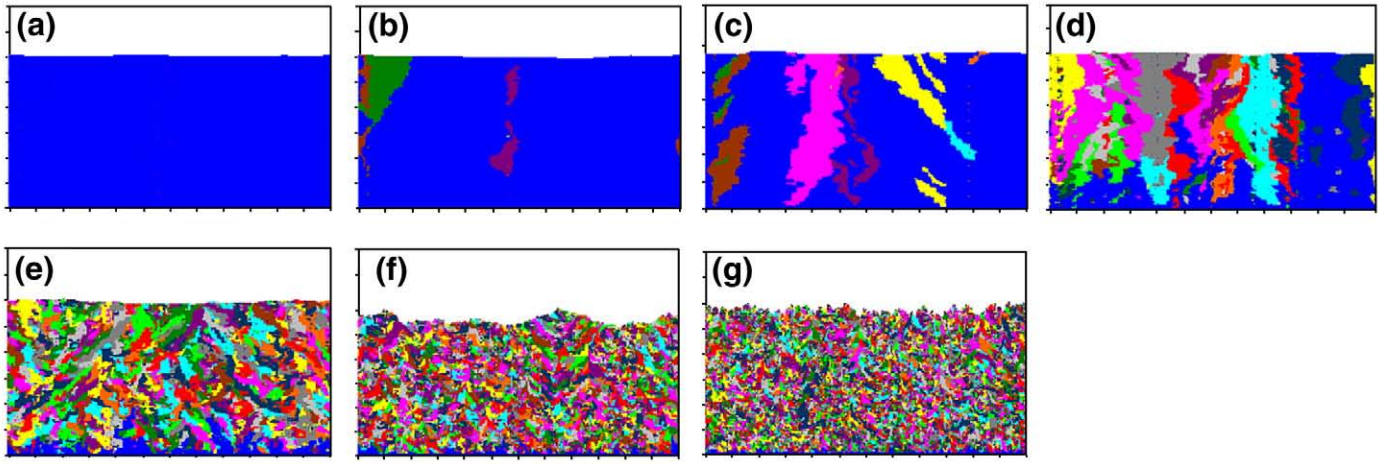

Fig. 8. Simulations of grain formation in CVD diamond films using the conditions given in Table 1 but with P_{renucl} having values: (a) 0, (b) 0.000001, (c) 0.00001, (d) 0.0001, (e) 0.001, (f) 0.01, and (g) 0.1.

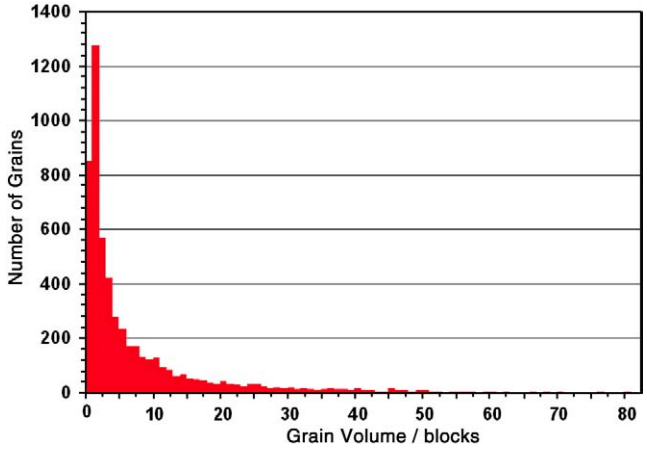

Fig. 9. Histogram of the grain size distribution obtained from Fig. 8(g).

epitaxially grown from the substrate have permeated up to 50 layers into the matrix before being overgrown by neighbouring grains. Again, we may compare this simulation with an electron micrograph cross-section from a nanocrystalline diamond film grown using high CH_4 content in the gas mix, shown in Fig. 7. Although the length scales are different, the clear similarities in structure, homogeneity and lack of columnar growth are recognisable in the real nanocrystalline film and the simulation.

The number of crystallites and their average size obviously depends upon the renucleation probability, P_{renucl}. This trend can be seen in Fig. 8 where the film morphology changes from single crystal diamond (SCD) for $P_{renucl} = 0$, to SCD containing large domains of other defects when $P_{renucl} \leq 0.00001$, then to a homogeneous film with roughly equal-sized grains spread uniformly throughout the film for $P_{renucl} > 0.00001$. These homogeneous films resemble the cauliflower diamond morphology seen in experiment. For $P_{renucl} \sim 0.1$ the grain volume is now smaller than ~10 blocks, consistent with that for UNCD, assuming that a block represents a C atom in the grain.

The grain sizes in these simulated UNCD films all have a distribution of grain volumes similar to the one shown in Fig. 9. This histogram is centred at a grain volume of 2 blocks with a full-width half-maximum value of ~3 blocks, but with a tail extending out beyond 30–40 blocks. The distribution does not fit a Gaussian or Lorentzian function, but the curve for block volumes>2 can be fitted with some success to an exponential decay curve of the form $A\ \exp(-Bx)$ with $B \sim 0.1$ and A constant. Fig. 10 shows that the number of grains increases rapidly as P_{renucl} increases, whilst the mean grain volume (number of blocks per grain) decreases. Fig. 11 shows that both the growth rate and the RMS roughness of the surface increase rapidly as a function of P_{renucl} until it reaches a value of ~0.01, and thereafter increase more slowly. The growth rate eventually reaches the theoretical maximum value of 4.3 μm h^{-1} at

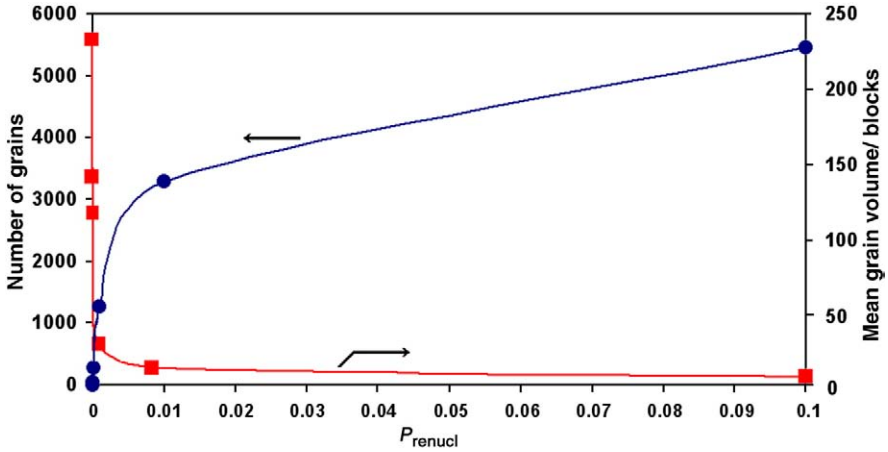

Fig. 10. Plot of the number of 2×2 grains in the 600×400 grid (blue circles) and the mean grain volume (red squares) as a function of P_{renucl} with all conditions as in Table 1.

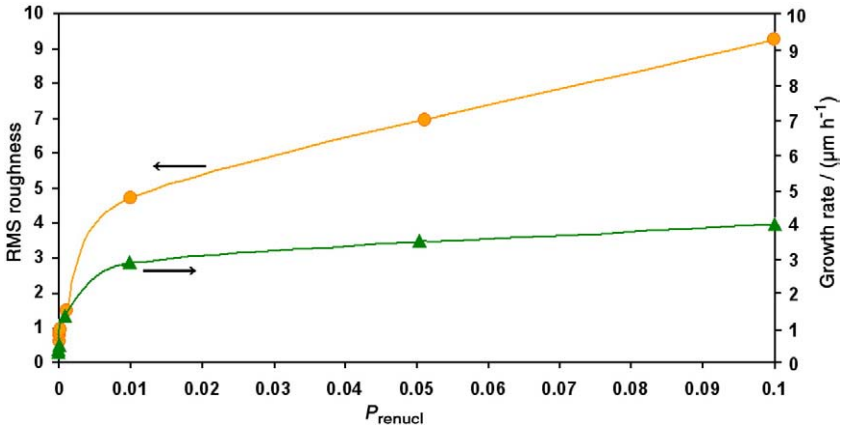

Fig. 11. RMS roughness in blocks (orange circles) and growth rate (green triangles) plotted as a function of P_{renucl}.

$P_{renucl} = 1$ when all carbons are utilised without loss, although by this point the RMS roughness is so high that the film has a random spiky morphology more associated with amorphous graphitic films than crystalline diamond layers. For $P_{renucl} < 0.001$ the film surface is smooth (RMS roughness < 1.5 blocks) but the growth rate is unrealistically small. This shows that under these conditions, the rate-limiting step for growth is the nucleation of a new layer. A small amount of renucleation is required in order to increase the growth rates to reasonable levels; however, too much causes roughening and degradation of the film morphology. An interesting observation is that the average grain diameter $\langle d \rangle$ shows a linear dependence with $1/\sqrt{P_{renucl}}$. The reason for this linear relationship is not clear, but it highlights that as the probability of forming surface defects increases, the average grain size decreases.

One final point that is worth investigating is the value of P_{below}, the probability that upon encountering a step-edge the migrating carbon species copy the underlying template of the lattice rather than that of the step-edge. The default value is 0.5, with equal probability for both. But Fig. 12 shows the effect of changing P_{below} to 0.1 and then to 0.9. For $P_{below} = 0.1$ the simulated film is composed of a layered structure of flat, horizontal grains. Conversely, for $P_{below} = 0.9$ the grains are now vertically aligned. Horizontal layered grains have never been reported in diamond CVD, whereas vertical grains are very similar to the columnar growth seen for MCD, and which can sometimes be seen on a nanoscale in NCD film cross-sections, for example in Fig. 7. We would therefore conclude that the true value for P_{below} should be somewhere between 0.5 and 0.9, although detailed *ab initio* modelling is required to ascertain this more accurately.

4. Conclusions

We have shown that, given reasonable values for the input parameters, a remarkably simple 1D MC model can reproduce many of the experimentally observed features of CVD diamond growth. Extension of this model to include multiple grain formation leads to realistic qualitative simulations for both columnar MCD growth as well as for homogeneous NCD and UNCD growth. The parameter controlling the crystallite size distribution is simply the probability that a moving C species creates an immobile, unetchable surface defect which then acts as a critical nucleus, either for the growth of the new layer or for the creation of a new defective crystallite misoriented with respect to the underlying layer. For high probabilities of renucleation that produce large numbers of small grains, the grain morphology was complex. Although they appeared to be on average spherical, the grains were, in fact, complicated 2D shapes forming an interconnected network throughout the entire structure. In a real film, these grains would form 3D networks. This has implications for the electronic properties of these films, as conductivity of NCD films is known to depend upon current transport both through the grains as well as around the grains via conducting grain boundaries [30]. Such interconnected grain boundaries provide percolation pathways for

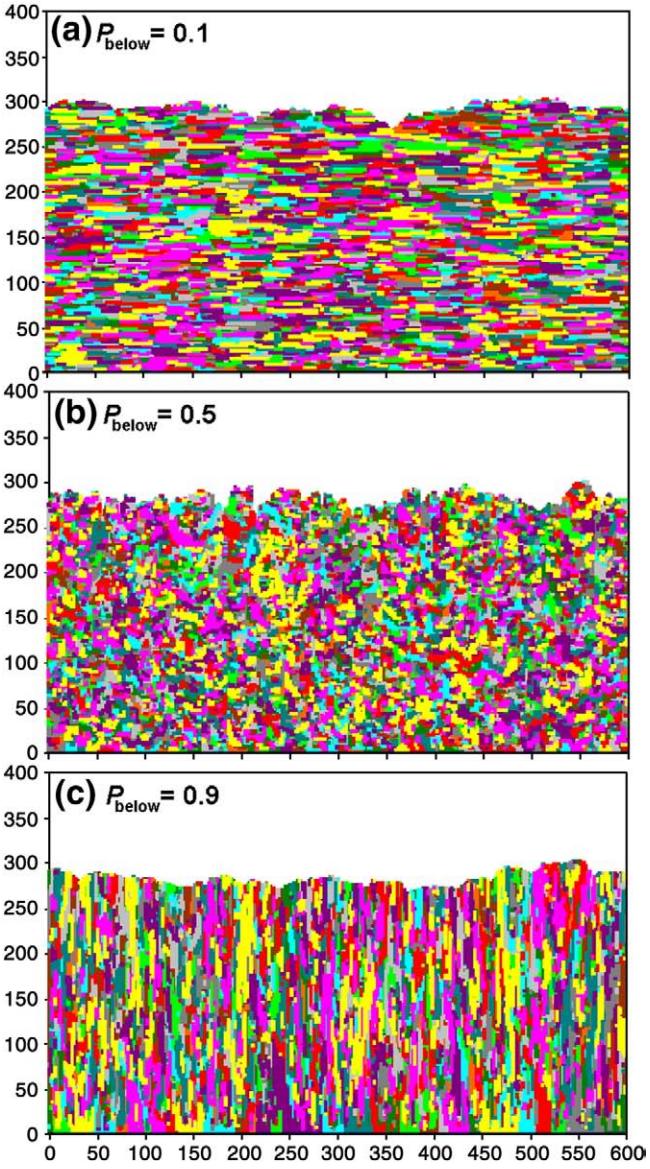

Fig. 12. Simulated film cross-sections using the standard values in Table 1 except with different values for P_{below}: (a) 0.1, (b) 0.5, and (c) 0.9.

current to flow through the film, and this may have implications for devices based on conducting NCD which rely on separated contacts, such as field emission devices.

A useful feature of a simple MC model such as this is that it can reveal gaps in our knowledge, as well as suggest areas where more work needs to be done. In particular, we highlight the following two points in order to stimulate more detailed theoretical studies.

(a) The two probabilities used to model surface defects, $P_{\text{dir-def}}$ and $P_{\text{jump-def}}$, are poorly understood. The value of $P_{\text{dir-def}}$ would depend upon the identity of the reactive adsorbate, for example atomic C, CH, or CN, and upon which type of site it was adsorbed (monoradical or biradical). We have made no attempt to distinguish between different reactive adsorbates or sites, and allocated the same probability to each. But a more detailed model would need to consider each possible defect-causing species in turn, along with their relative concentrations near the surface. The value of $P_{\text{jump-def}}$ is more critical, since this is tested at every time-step, yet its value, too, is little more than an educated guess. Detailed *ab initio* calculations need to be made to ascertain what defects (if any!) are possible when a migrating CH_2 bridging-group bonds 'crookedly', and of the energies associated with these defects.

(b) The parameter P_{below} was used to determine whether C species landing next to a step-edge (which may be a surface defect) templated on the underlying lattice or on the step-edge. This parameter, too, is unknown, and a value of 0.5 was chosen as default. However, this value critically determines the crystallite morphology, with $P_{\text{below}}<0.5$ giving horizontally layered grains, $P_{\text{below}}=0.5$ giving roughly spherical grains, and $P_{\text{below}}>0.5$ giving vertically aligned columnar grains. The latter most closely resemble the types of grains resulting from growth conditions between those for NCD and MCD, and we therefore concluded that a more realistic value for P_{below} is between 0.5 and 0.9. Theoretical studies, using, say, *ab initio* methods may be able to obtain a more accurate estimate for P_{below}, as well as to put this model on a more sound theoretical footing.

There are some obvious extensions to this work which we are in the process of implementing. At present, the probabilities for the various reactions and processes have independent values. In a future publication these probabilities will be related to experimental parameters, such as substrate temperature or H atom concentration. The MC model should then be able to make predictions about the effect of different growth conditions upon the growth rate, morphology and growth mechanism in real systems.

We also intend to extend the program to include aspects of the gas-surface processes consistent with our model of diamond growth that was discussed in the Introduction and detailed in Refs. [18,21,22]. This would involve adding routines which differentiate between adsorption onto and desorption/etching from monoradical and biradical sites, and for different adsorbing species. Some of these processes would be dependent upon the concentrations of gas phase H and CH_3 as well as the local gas and surface temperatures.

Acknowledgments

The authors wish to thank Neil Fox, Keith Rosser, Ben Truscott, Walther Schwarzacher, and Jeremy Harvey for useful discussions and suggestions, and Dierk Raabe of the Max-Planck-Institut für Eisenforschung and John Wiley publishers for permission to use Fig. 3.

References

[1] P.W. May, Science 319 (2008) 1490.
[2] S. Prawer, A.D. Greentree, Science 320 (2008) 1601.
[3] C.E. Nebel, B. Rezek, D. Shin, H. Uetsuka, N. Yang, J. Phys. D: Appl. Phys. 40 (2007) 6443.
[4] F.A.M. Koeck, R.J. Nemanich, Diamond Relat. Mater. 18 (2009) 232.
[5] P.W. May, Philos. Trans. R. Soc. Lond., A 358 (2000) 473.
[6] O.A. Williams, M. Daenen, J. D'Haen, K. Haenen, J. Maes, V.V. Moshchalkov, M. Nesládek, D.M. Gruen, Diamond Relat. Mater. 15 (2006) 654.
[7] P.W. May, J.N. Harvey, J.A. Smith, Yu.A. Mankelevich, J. Appl. Phys. 99 (2006) 104907.
[8] D.M. Gruen, O.A. Shenderova (Eds.), Synthesis, Properties and Applications of Ultrananocrystalline Diamond, A.Ya. Vul' (Ed.), NATO Science Series part II, vol. 192, Springer, 2005.
[9] G. Bogdan, K. De Corte, W. Deferme, K. Haenen, M. Nesládek, Phys. Status Solidi, A Appl. Res. 203 (2006) 3063.
[10] J. Isberg, J. Hammersberg, E. Johansson, T. Wikström, D.J. Twitchen, A.J. Whitehead, S.E. Coe, G.A. Scarsbrook, Science 297 (2002) 1670.
[11] C.-S. Yan, H.-K. Li, W. Mao, J. Qian, Y. Zhao, R.J. Hemley, Phys. Status Solidi, A Appl. Res. 201 (2004) R25.
[12] S.S. Ho, C.S. Yan, Z. Liu, H.K. Mao, R.J. Hemley, Ind. Diamond Rev. 28 (January 2006).
[13] D.G. Goodwin, J.E. Butler, in: M.A. Prelas, G. Popovici, L.K. Bigelow (Eds.), Handbook of Industrial Diamonds and Diamond Films, Marcel Dekker, New York, 1998.
[14] S.J. Harris, Appl. Phys. Lett. 56 (1990) 2298.
[15] J.E. Butler, R.L. Woodin, L.M. Brown, P. Fallon, Philos. Trans. R. Soc. Lond., Phys. Sci. Eng. 342 (1993) 209.
[16] J.E. Butler, I. Oleynik, Phil. Trans. Roy. Soc. A 366 (2008) 295.
[17] D. Das, R.N. Singh, Int. Mater. Rev. 52 (2007) 29.
[18] P.W. May, Yu.A. Mankelevich, J. Phys. Chem. C 112 (2008) 12432.
[19] S. Skokov, B. Weiner, M. Frenklach, J. Phys. Chem. 98 (1994) 7073.
[20] J.C. Richley, J.N. Harvey, M.N.R. Ashfold, J. Phys. Chem. A 113 (2009) 11416.
[21] P.W. May, M.N.R. Ashfold, Yu.A. Mankelevich, J. Appl. Phys. 101 (2007) 053115.
[22] Yu.A. Mankelevich, P.W. May, Diamond Relat. Mater. 17 (2008) 1021.
[23] P.W. May, N.L. Allan, J.C. Richley, M.N.R. Ashfold, Yu.A. Mankelevich, J. Phys. Cond. Matter 21 (2009) 364203.
[24] A. Cheesman, PhD Thesis, "Investigations into the fundamentals of gas-phase and gas-surface chemistry prevalent in growth of Chemical Vapour Deposited diamond films", School of Chemistry, Bristol University, UK, July 2006.
[25] P.W. May, Yu.A. Mankelevich, J. Appl. Phys. 100 (2006) 024301.
[26] R.S. Tsang, C.A. Rego, P.W. May, M.N.R. Ashfold, K.N. Rosser, Diamond Relat. Mater. 6 (1997) 247.
[27] A. Pimpinelli, J. Villain, Physics of Crystal Growth, Cambridge University Press, Cambridge, U.K., 1998
[28] T. Liu, D. Raabe, W. Mao, S. Zaefferer, Adv. Funct. Mater. (in press); doi:10.1002/adfm.200901231.
[29] T. Liu, D. Raabe, Appl. Phys. Lett. 94 (2009) 021119.
[30] P.W. May, W.J. Ludlow, M. Hannaway, P.J. Heard, J.A. Smith, K.N. Rosser, Diamond Relat. Mater. 17 (2008) 105.